Analytica Chimica Acta xxx (2018) 1–8

Contents lists available at ScienceDirect

Analytica Chimica Acta

journal homepage: www.elsevier.com/locate/aca

Label- and enzyme-free detection of glucose by boronic acid-coupled poly(styrene-*b*-acrylic acid) at liquid crystal/aqueous interfaces

Sundas Munir, Soo-Young Park*

School of Applied Chemical Engineering, Polymeric Nano Materials Laboratory, Kyungpook National University, Daegu, 41566, Republic of Korea

HIGHLIGHTS

- A glucose biosensor was developed based on a 4-cyano-4′-pentylbiphenyl (5CB)-filled transmission electron microscopy (TEM) grid cell by coating poly (styrene-*b*-acrylic acid) (PS-*b*-PAA) at the 5CB/aqueous interface and immobilising 3-aminophenyl boronic acid (APBA) on the PAA block chains by *N*-(3-dimethylaminopropyl)-*N*-ethyl-carbodiimide coupling.
- Binding events between APBA and glucose were translated into homeotropic-to-planar configurational changes of 5CB, which were observed by polarised optical microscopy (POM) under crossed polarisers.
- This liquid-crystal-based glucose biosensor exhibited high sensitivity (limit of detection: 0.1 mM), even in complex serum and urine samples, high selectivity (against cholesterol, haemoglobin, and urea), and good stability for 40 d.
- This new and sensitive glucose biosensor has the advantages of low production cost, a simple immobilisation technique, and easy detection with POM, and may be useful for pre-screening glucose levels in human samples (serum and urine).

GRAPHICAL ABSTRACT

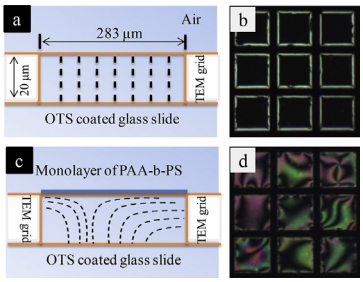

Abbreviations: APBA, 3-aminophenyl boronic acid; 5CB, 4-cyano-4′-pentylbiphenyl; EDC, *N*-(3-dimethylaminopropyl)-*N*-ethylcarbodiimide; GI, grey-scale intensity; H-P, homeotropic-to-planar; LB, Langmuir–Blodgett; LC, liquid crystal; LCP-*b*-PAA, poly(4-cyanobiphenyl-4′-undecylacrylate-*b*-acrylic acid); NHS, *N*-hydroxysulfosuccinimide; NE, non-enzymatic; OTS, octadecyltrichlorosilane; PBS, Phosphate buffer solution; PMAA, poly(methyl methacrylate); POM, polarised optical microscopy; PS-*b*-PAA, poly(styrene-*b*-acrylic acid); TEM, transmission electron microscopy; NE, non-enzymatic; LC, liquid crystal; LCP-*b*-PAA, poly(4-cyanobiphenyl-4′-undecylacrylate-*b*-acrylic acid); PS-*b*-PAA, poly(styrene)-*b*-poly(acrylic acid); TEM, transmission electron microscopy; 5CB, 4-cyano-4′-pentylbiphenyl; LB, Langmuir–Blodgett; APBA, 3-aminophenyl boronic acid; EDC, *N*-(3-dimethylaminopropyl)-*N*-ethylcarbodiimide; H-P, homeotropic-to-planar; PBS, phosphate buffer solution; OTS, octadecyltrichlorosilane; NHS, *N*-hydroxysulfosuccinimide; GI, grey-scale intensity; PMAA, poly(methyl methacrylate); C_g, glucose concentration.

* Corresponding author.
E-mail address: psy@knu.ac.kr (S.-Y. Park).

https://doi.org/10.1016/j.aca.2018.05.039

ARTICLE INFO

Article history:
Received 12 March 2018
Received in revised form
5 May 2018
Accepted 12 May 2018
Available online xxx

Keywords:
Non-enzymatic biosensor
Liquid crystal
Polyelectrolyte brush
3-Aminophenyl boronic acid
Glucose

ABSTRACT

A glucose biosensor was developed based on a 4-cyano-4′-pentylbiphenyl (5CB)-filled transmission electron microscopy (TEM) grid cell by coating poly (styrene-*b*-acrylic acid) (PS-*b*-PAA) at the 5CB/aqueous interface and immobilising 3-aminophenyl boronic acid (APBA) on the PAA block chains by *N*-(3-dimethylaminopropyl)-*N*-ethylcarbodiimide coupling. Binding events between APBA and glucose were translated into homeotropic-to-planar configurational changes of 5CB, which were observed by polarised optical microscopy (POM) under crossed polarisers. This liquid-crystal-based glucose biosensor exhibited high sensitivity (limit of detection: 0.1 mM), even in complex serum and urine samples, high selectivity (against cholesterol, haemoglobin, and urea), and good stability for 40 d. This new and sensitive glucose biosensor has the advantages of low production cost, a simple immobilisation technique, and easy detection with POM, and may be useful for pre-screening glucose levels in human samples (serum and urine).

1. Introduction

Diabetes mellitus, commonly referred to as diabetes, is a group of metabolic disorders in which the blood sugar level increases or decreases relative to the normal value of 80–120 mg dL^{-1} (4.4–6.6 mM) over a prolonged period [1]. Symptoms of hyperglycaemia (high blood sugar) include frequent urination, increased thirst, and hunger, whereas those of hypoglycaemia (low blood sugar) include sweating, nervousness, weakness, dizziness, blurred vision, and headache. If left untreated, diabetes can cause many long-term complications, such as cardiovascular disease, stroke, chronic kidney disease, foot ulcers, and damage to the eyes. Acute complications can include diabetic ketoacidosis, hyperosmolar hyperglycaemic state, or death [2,3]. A plethora of reports has been published on the detection of glucose. Various techniques, including electrochemical, potentiometric, amperometric, and optical (colorimetric or fluorescent) methods, have been utilised to sense glucose levels in human samples. These techniques usually utilise enzymes (e.g., glucose oxidase, horseradish peroxidase, and D-glucono-δ-lactone) to achieve highly specific detection of glucose. For optical sensors, labelling of biomolecules with different enzymes or optical tags, such as dyes, adds complexity, increases cost, leads to poor stability and reproducibility, and makes practical bedside diagnostics difficult.

Although enzyme-based biosensors exhibit high sensitivity and specificity, their applications are limited by drawbacks such as sophisticated immobilisation techniques, enzyme stabilisation protocols, and hindrance of enzyme activity by long-term exposure to high pH, high temperature, humid environments, toxic chemicals, etc. [4,5]. Thus, there is considerable demand for glucose detection methods based on alternative non-enzymatic (NE) compounds. The most studied NE compounds are boronic acid derivatives that covalently bind glucose [4,6]. In addition, various metallic compounds (e.g., Pt and Au) and transition metal oxides (NiO, Co_3O_4, CuO, and TiO_2) have been utilised for highly sensitive screening of glucose [6,7]. These NE approaches also show high sensitivity and stability for glucose sensing. However, electrode preparation is complex and time-consuming, requiring sophisticated and complex procedures.

Over the last 20 years, liquid crystal (LC)-based biosensors have been utilised for label-free sensing of various biomolecules by several research groups [8–11]. The detection of biomolecules, such as deoxyribonucleic acid, glucose, cholesterol, urea, proteins, and avidin, by the nematic [12] and chiral nematic phases [13] of thermotropic mesogens at the interface with an immiscible aqueous solution [12–22] has been reported. LC materials respond to and amplify small changes in pH, temperature, shear, and electric (or magnetic) fields [23]. LC molecules have the ability to change their orientations owing to the adsorption or desorption of molecules at the interface and in response to stimuli. These changes can be observed and reported in real time by following changes in the optical birefringence of the LC. As LC materials possess very low interfacial energies (10^{-6}–10^{-3} J m^{-2}) at the interfaces formed with immiscible aqueous solutions, they are quite sensitive to environmental changes through an ordering transition, which can be propagated to a distance of ~100 μm (molecular length of 10^5) [24].

In previous studies, our group utilised poly (4-cyanobiphenyl-4′-undecylacrylate-*b*-acrylic acid) (LCP-*b*-PAA) to translate different phenomena (e.g., shrinking or swelling of PAA chains as a result of an enzymatic reaction or adsorption/desorption of materials) occurring at LC/aqueous interfaces [25–27]. Because of the miscibility of the LCP block with the LC hosted on a flat (e.g., transmission electron microscopy (TEM) grid cell) or spherical substrate (e.g., microdroplets), the phenomena occurring at these interfaces were effectively transduced. However, the use of non-commercial LCP-*b*-PAA is limited by the multistep synthesis required for block copolymerisation and the expensive starting materials. These drawbacks motivated us to utilise an alternative commercially available amphiphilic material that can effectively and potently translate interfacial phenomena to the LC. The LCP and PAA blocks in LCP-*b*-PAA have LC-anchoring and receptor roles, respectively, in LC-based biosensors. Among commercially available block copolymers, poly (styrene)-*b*-poly (acrylic acid) (PS-*b*-PAA) may exhibit similar properties because the PS block has good potential for LC anchoring owing to its hydrophobicity.

In this study, we examined the assembly of PS-*b*-PAA at the interface between a 4-cyano-4′-pentylbiphenyl (5CB)-coated TEM grid and water using Langmuir–Blodgett (LB) device, as well as the glucose sensing performance of this system. To record the compression isotherm for PS-b-PAA residing at the air (gas)/water interface, the small quantity (2 mg mL^{-1}) of the PS-b-PAA was dissolved completely in a mixture of volatile solvents (toluene and dioxane) and was then carefully applied via micropipette (200 μL) onto a clean water surface taken into the LB trough. Following evaporation of the solvents, the film compression was started by movement of the mobile barriers. This results in an increase in surface pressure which was recorded. The PS-*b*-PAA layer was then functionalised with a NE 3-aminophenyl boronic acid (APBA) moiety by *N*-(3-dimethylaminopropyl)-*N*-ethylcarbodiimide (EDC) coupling. The APBA-functionalised PS-*b*-PAA assembled at the 5CB/aqueous interface in the TEM grid ($TEM_{PAA\text{-}APBA}$) was utilised for glucose sensing by following the homeotropic-to-planar (H-P)

Please cite this article in press as: S. Munir, S.-Y. Park, Label- and enzyme-free detection of glucose by boronic acid-coupled poly(styrene-*b*-acrylic acid) at liquid crystal/aqueous interfaces, Analytica Chimica Acta (2018), https://doi.org/10.1016/j.aca.2018.05.039

change of the molecular alignment of 5CB that occurred with reversible covalent bonding between APBA and glucose. This binding interaction lowered the local pH of the medium, which caused shrinking (protonation) of the PAA chains and led to the H-P transition. This label- and enzyme-free LC platform may provide a new avenue for selective and cost-effective sensing of glucose levels in human samples, such as blood and urine.

2. Materials and methods

2.1. Materials and instruments

Microscope glass slides (Duran Group, Germany) were cleaned with piranha solution to remove organic contaminants (caution: this solution reacts violently with organic materials and may explode, therefore proper care is necessary), washed with distilled water, and then dried under nitrogen. Copper TEM specimen grids (G75, grid hole width: 285 μm, pitch: 340 μm, bar width: 55 μm, diameter: 3.05 mm, and thickness: 18 μm) were purchased from Ted Pella Inc. 5CB (TCI, Japan). Phosphate buffer solution (PBS; Duksan, Korea), octadecyltrichlorosilane (OTS), APBA, (3-dimethylaminopropyl)-*N*-ethylcarbodiimide hydrochloride (EDC·HCl), *N*-hydroxysulfosuccinimide (NHS), cholesterol, urea, and haemoglobin were purchased from Sigma-Aldrich (United Kingdom). Milli-Q water (resistivity > 18.2 MΩ cm) was used in all experiments. PS-*b*-PAA (Polymer Source, Canada) had a number-average molecular weight of PS(2.8 k)-*b*-PAA (10 k), where the numbers represent the number-average molecular weight of each block in 1000 g mol^{-1}. The urine samples, which did not contain glucose, were collected from a healthy donor (volunteer). These fluids were spiked with glucose and used as the test samples. Images and videos were captured using a charge-coupled device camera (STC-TC83USB, Samwon, Korea) connected to a polarised optical microscope (ANA-006, Leitz, Germany). The grey-scale intensity (GI) values of the frames were obtained from (equation (1)) using Adobe Photoshop CS5 software.

$$GI = \frac{\left(\varphi_o - \varphi_f\right)}{\varphi_0} \times 100 \quad (1)$$

Where φ_o and φ_f are the GI of the TEM_{PAA} sensor at the reference homeotropic or planar and after the glucose reaction or exposure to pH solution, respectively. To characterise the covalent bonding between APBA and PAA chains using FTIR spectroscopy (FT/IR–620 spectrometer, Jasco, Japan), aqueous solutions were collected at different stages during the preparation of $TEM_{PAA\text{-}APBA}$. The samples for FTIR analysis were dried using a freeze dryer (FD 1000, EYELA, Japan) and pelletised with KBr.

2.2. PS-b-PAA layer formation

A PS-*b*-PAA layer was formed using an LB KSV layer builder (AAA100178, KSV Instruments, Ltd., Finland) connected to a KSV mini-micro trough, which was surrounded by an environmental chamber. The working area of the trough was 17 × 5 cm^2. The surface pressure of the layer at the air/liquid interface was measured using a Wilhelmy plate attached to a microbalance. All experiments were performed at room temperature. PS-*b*-PAA in a mixed solvent of toluene and dioxane was used for layer formation. First, PS-*b*-PAA was dissolved in dioxane and kept at 60 °C for 2 d. Toluene was then added to the dioxane solution to obtain a final concentration of 2 mg mL^{-1} with a dioxane-to-toluene ratio of 6:4 (v/v). When a zero surface pressure was reached, 200 μL of the PS-*b*-PAA solution was spread on a water subphase to form a layer and then left for 1 h. The layer was compressed at a rate of 5 mm min^{-1} to achieve the desired surface pressure of 35 m Nm^{-1}.

2.3. Preparation of the sensor

A polydimethylsiloxane flow cell was fabricated using the method reported in our previous studies [10,15]. Microscope glass slides were cleaned and coated with OTS to align 5CB homeotropically on the surface. A copper TEM grid was placed on the surface of the 12 × 8 mm^2 OTS-coated glass. This glass was glued to another glass slide with epoxy resin. A 1 μL drop of 5CB was placed on the TEM grid using a syringe. Excess 5CB was removed with a capillary tube to obtain a thin uniform film. The PS-*b*-PAA layer was transferred to the 5CB-filled TEM grid using the following method. The 5CB-filled TEM grid was placed slowly onto the PS-*b*-PAA layer in the LB trough, with the TEM grid side downward, coming to rest on a silicone spacer (2 mm thick) attached to another glass slide in the LB bath. The two glass slides spaced with silicone rubber were then clipped together with binder clips. The inlet and outlet ports for exchanging solutions were made by punching needles through the silicone rubber. The internal volume of the flow cell was 0.4 mL. Different APBA aqueous solutions (0.1, 0.2, 0.5, and 1 wt%) prepared in PBS 8 were used to immobilise APBA on the PAA chains by the following method. Briefly, the PAA chains were activated with 0.2 wt% EDC·HCl:NHS for 2 h. Then, the APBA solution was introduced into the flow cell, which was then maintained at room temperature for 12 h.

3. Results and discussion

The molecules of 5CB hosted on the TEM grid cell initially exhibited a homeotropic (perpendicular) alignment, which was achieved by using an OTS coating on the glass, as shown in Fig. S1a and b. After transferring the layer using the LB device, the mesogens were observed under crossed polarisers to have a parallel alignment owing to the adsorption of PS-*b*-PAA at the LC/aqueous interface, as shown in Fig. S1c and d. The bright colour observed in the TEM cell in the polarised optical microscopy (POM) image corresponds to the continuous change of the director profile of 5CB from homeotropic (bottom of the OTS-coated glass) to parallel (interface between 5CB and water).

3.1. pH response of TEM_{PAA}

A basic requirement for a glucose biosensor using APBA is pH responsiveness. The pH-dependent response of PAA-*b*-LCP at the LC/water interface was studied with TEM grid cells, and a P-H transition was observed with increasing pH in water [16,20]. The change in the orientation of 5CB with increasing pH in water is due to the high anionic charge density resulting from deprotonation of the PAA chains. The response of LC microdroplets coated with PAA-*b*-LCP to changes in pH has also been investigated [28]. A bipolar (planar) to radial (homeotropic) orientational change occurred with increasing pH [24,29]. These results indicate that the dissociation behaviour of PAA is one of the main mechanisms for LC orientational changes. The dissociation behaviour of the PAA chain in the brush is complicated and depends on various factors including pH, salt concentration, and grafting density [30,31]. Currie et al. reported that the PAA brush thickness as a function of the ionic strength is non-monotonic at a given pH and grafting density. Further, they reported that the swelling increases with increasing pH and grafting density. At pH 3 (far below the pK_a of PAA), the brush height is independent of the ionic strength because the fraction of dissociated monomers is close to zero, regardless of the ionic strength. At higher pH, the brushes swell with increasing

Please cite this article in press as: S. Munir, S.-Y. Park, Label- and enzyme-free detection of glucose by boronic acid-coupled poly(styrene-*b*-acrylic acid) at liquid crystal/aqueous interfaces, Analytica Chimica Acta (2018), https://doi.org/10.1016/j.aca.2018.05.039

ionic strength because of an increasing fraction of charged monomers [32]. Dong et al. determined the degree of dissociation of both PAA and poly (methyl methacrylate) (PMAA) brushes at different pH using FTIR spectroscopy. They acquired the FTIR spectra for a series of PAA and PMAA brushes treated with different buffer solutions. At low pH (pH < 4), the carboxylic acid groups in the brushes are protonated and show the characteristic C=O (of COOH) stretching peak at around 1732 cm^{-1}. At high pH, the intensity of the asymmetric COO^- stretching peak at 1550 cm^{-1} increases with increasing pH [33], owing to deprotonation of COOH groups. Previous studies also revealed that an increase in the charge density of PAA chains causes homeotropic orientation of 5CB in the TEM grid cell [12].

The pH response of TEM_{PAA} was tested by alternating between PBS solutions at pH 5 and 8, as shown in Fig. 1. Changing the pH from 5 to 8 triggered the P-H transition, whereas changing from pH 8 to 5 triggered the H-P transition. At pH 5, the brushes of PAA on TEM_{PAA} were in the collapsed form, causing the planar alignment, as demonstrated in Fig. 1a(i, iii, v, vii, and ix). In contrast, by changing the pH from 5 to 8, the homeotropic alignment was observed, as shown in Fig. 1(ii, iv, vi, vii, and x). This transition of the director orientation can be attributed to the deprotonation (and protonation) of the PAA chains, as mentioned previously. This reversible change was successfully observed over 5 cycles. Although further tests were not performed, we believe that the reversible behaviour will continue in further cycles. These observations suggest that the change observed in Fig. 1 is mediated by the pH-dependent response of PAA assembled at the interface. The plot of the average GI values for TEM_{PAA} as a function of cycle (Fig. 1b) illustrates the reversible pH-dependent transition between the planar and homeotropic orientations. The observation of constant GI values with cycling indicates that TEM_{PAA} is quite stable, with the original state of TEM_{PAA} maintained during repeated experiments.

The carboxylic groups of PAA were activated by using 0.2 wt% EDC·HCl:NHS (4:1, mol ratio) as a coupling agent, after which APBA was immobilised onto the PAA chains at pH = 8. The planar orientation was maintained after activation with EDC (Fig. 2a(i)). Subsequent immobilisation of 0.5 wt% APBA changed the orientation from planar to homeotropic (Fig. 2a(ii)). This homeotropic orientation is due to the charged state of PAA chains at pH = 8. Various concentrations of APBA (C_{APBA}) were tested at pH = 8 to determine the concentration at which the performance of the $TEM_{PAA\text{-}APBA}$ sensor was optimized. Fig. 2a(iii–vii) shows POM images of $TEM_{PAA\text{-}APBA}$ prepared at different C_{APBA} after the addition of 1 mM glucose. The initial homeotropic orientation of the $TEM_{PAA\text{-}APBA}$ sensor prepared at C_{APBA} = 0.005 wt% (Fig. 2a(iii)) was maintained after the addition of 1 mM glucose, indicating that the extent of glucose/APBA binding at this concentration was not sufficient to change the ordering of 5CB. When C_{APBA} was increased to 0.01 wt% (Fig. 2a(iv)), some bright domains started to appear. Birefringent colour was observed over the whole TEM grid when C_{APBA} was 0.05–0.5 wt% (Fig. 2a(v–vii)). Thus, 0.2 wt% APBA in aqueous solution was utilised to prepare $TEM_{PAA\text{-}APBA}$ sensors for further experiments.

Covalent bonding of APBA with PS-*b*-PAA was confirmed using

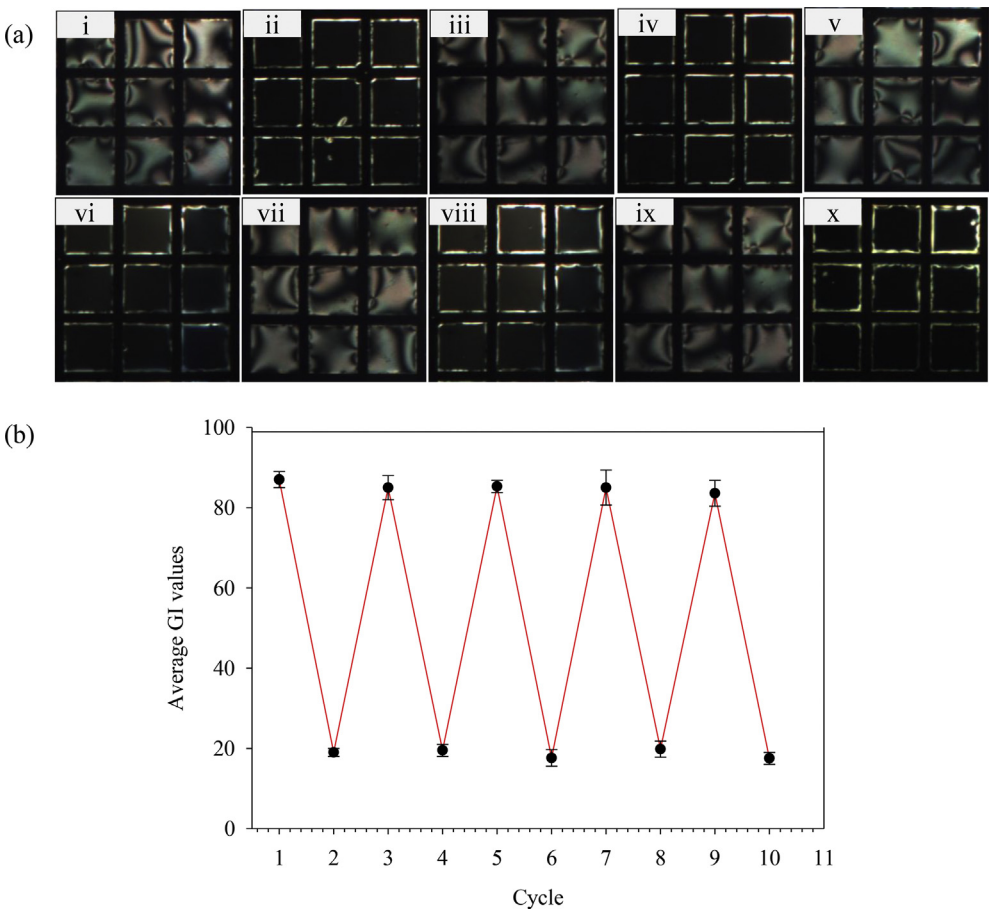

Fig. 1. (a) POM images of the TEM_{PAA} when alternately exposed to PBS solutions at pH 5 (i, ii, v, vii, and ix) and 8 (ii, iv, vi, vii, and x), and (b) their average GI values of (a) as a function of cycle .

Please cite this article in press as: S. Munir, S.-Y. Park, Label- and enzyme-free detection of glucose by boronic acid-coupled poly(styrene-*b*-acrylic acid) at liquid crystal/aqueous interfaces, Analytica Chimica Acta (2018), https://doi.org/10.1016/j.aca.2018.05.039

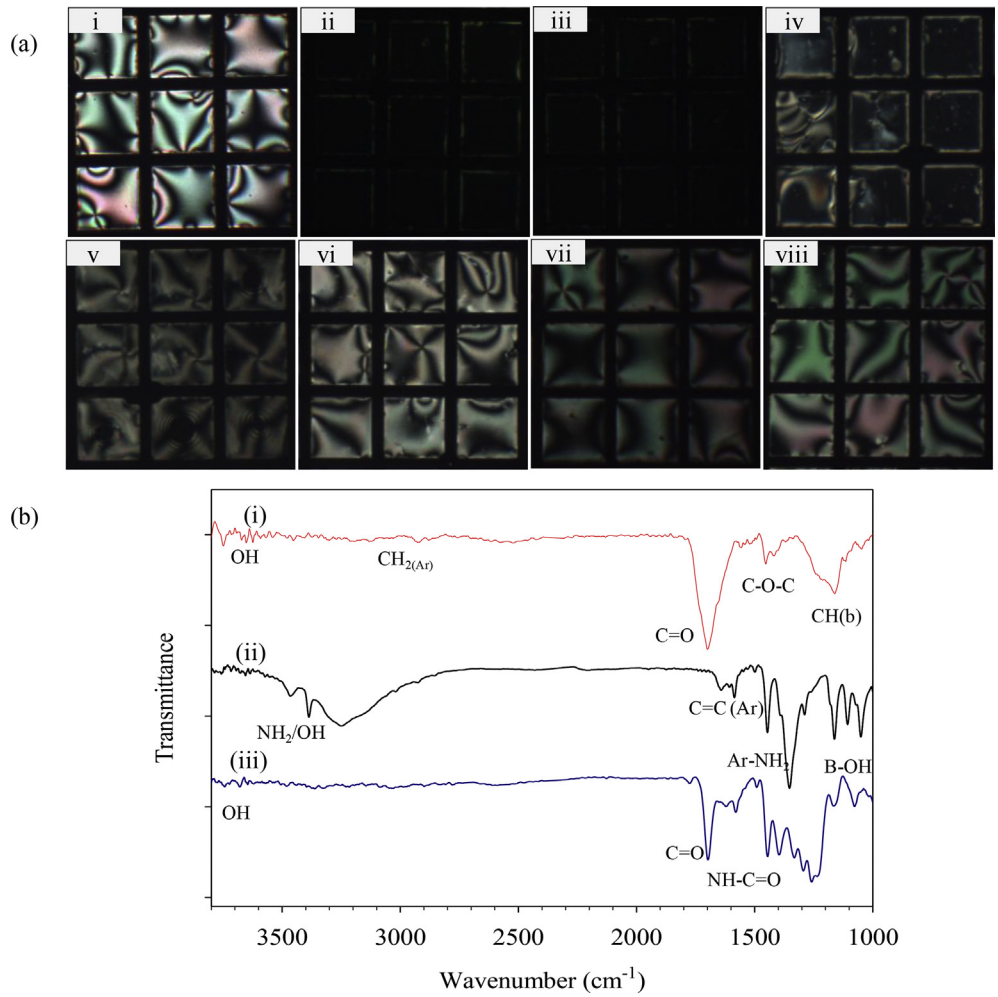

Fig. 2. (a) POM images of (i) TEM_{PAA} after activation of PAA chains with EDC·HCl and NHS, (ii) TEM $_{PAA-APBA}$ prepared at $C_{APBA} = 0.5$ wt% before addition of 1 mM of glucose, and TEM $_{PAA-APBA}$ prepared at C_{APBA} = (iii) 0.005, (iv) 0.01, (v) 0.05, (vi) 0.1, (vii) 0.2, and (vii) 0.5 wt % after addition of 1 mM of glucose, and (b) FTIR spectra of the (i) PS-b-PAA, (ii) APBA, and (iii) PS-b-PAA-APBA.

FTIR spectroscopy, as shown in Fig. 2b. The FTIR spectrum of PS-*b*-PAA has peaks at 3300 and 1600 cm^{-1}, which are attributable to O—H and C=O stretching, respectively, of PAA (Fig. 2b(i)). The FTIR spectrum of APBA has characteristic peaks at 1276, 1506, 3300, and 3429 cm^{-1}, which correspond to B—OH stretching vibrations, C—B vibrations, $C{=}C_{(aromatic)}$ stretching, and OH/NH_2 stretching, respectively (Fig. 2b(ii)). The FTIR spectrum of PS-*b*-PAA-APBA exhibits distinctive peaks at 1550 and 1650 cm^{-1} corresponding to amide-I and -II bonds, respectively, and peaks at 1709 and 3600 cm^{-1} attributed to C=O and O—H stretching, respectively (Fig. 2b(iii)). Thus, amide bonds were formed by EDC coupling between PAA and APBA, confirming successful covalent bonding of APBA with PS-*b*-PAA.

3.2. Sensitivity of $TEM_{PAA-APBA}$ for glucose detection

Reversible binding occurs between APBA and glucose, as shown in Scheme 1 [34]. The protons generated by this reaction decrease the local pH of the system and induce the protonation of the PAA chains, resulting in the H-P transition. Fig. 3 exhibits the response of the $TEM_{PAA-APBA}$ sensor to different glucose concentrations (C_g). The initial homeotropic orientation (Fig. 2a(ii)) does not change at $C_g = 0.01$ and 0.05 mM (Fig. 3a(i and ii)). At $C_g = 0.1$ mM (Fig. 3a(iii)), the homeotropic orientation of 5CB changes to a planar configuration. When C_g increases to 0.2 mM (Fig. 3a(iv)), more birefringence is observed. Thus, $TEM_{PAA-APBA}$ has a sensitivity of ~0.1 mM. Yao et al. reported a detection limit of 0.026 mM for

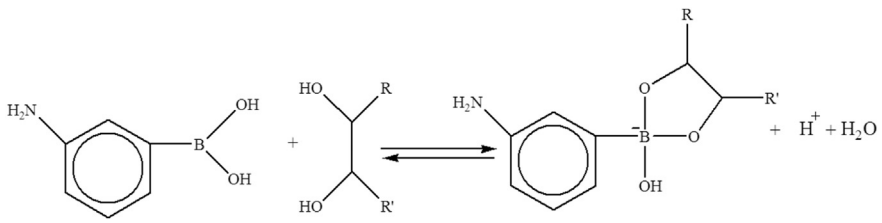

Scheme 1. Reversible binding between 3-APBA and glucose.

Please cite this article in press as: S. Munir, S.-Y. Park, Label- and enzyme-free detection of glucose by boronic acid-coupled poly(styrene-*b*-acrylic acid) at liquid crystal/aqueous interfaces, Analytica Chimica Acta (2018), https://doi.org/10.1016/j.aca.2018.05.039

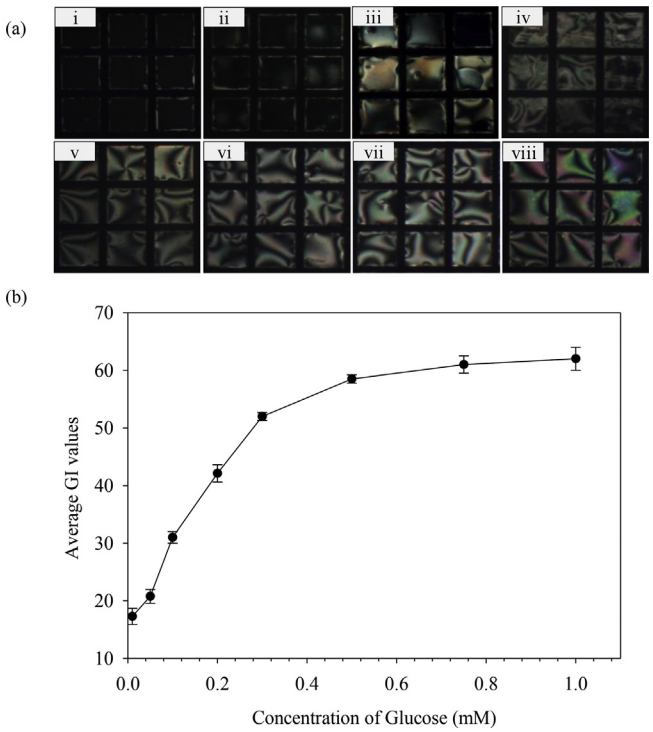

Fig. 3. (a) POM images of the $TEM_{PAA\text{-}APBA}$ when exposed to different C_gs of (i) 0.01, (ii) 0.05, (iii) 0.1, (iv) 0.2, (v) 0.3, (vi) 0.5, (vii) 0.75, and (vii) 1 mM and (b) their average GI values of (a) as a function of C_g.

glucose [35] by utilising colour-tuneable luminescent macrofibres based on cadmium telluride quantum dots, which were loaded in bacterial cellulose nanofibres prepared by wet spinning. Lee and colleagues reported a sensitivity of 1 mM for glucose [36,37] by using a poly (vinylidene fluoride)/poly (aminophenylboronic acid) composite nanofibrous membrane. Similarly, they reported a sensitivity of 0.16 mM for glucose by using polymer nanobeads deposited with copper nanoparticles [37]. Therefore, the detection limit of $TEM_{PAA\text{-}APBA}$ was nearly/almost comparable to those of other reported glucose biosensors.

This $TEM_{PAA\text{-}APBA}$ sensor, which can be fabricated at a low cost, is useful for detecting glucose in small amounts of sample because the volume needed for detection is only 0.4 mL. As shown in Fig. 3b, the average GI value continuously increases as C_g increases. The continuous increase of the GI value may indicate that the molecular tilting angle of 5CB in the TEM grid changes continuously with the addition of glucose.

3.3. Analysis of real samples and selectivity of $TEM_{PAA\text{-}APBA}$

The sensitivity of $TEM_{PAA\text{-}APBA}$ was examined with human serum samples diluted in PBS at pH 7, as shown in Fig. 4a. The tested serum sample had an initial C_g of 5.32 mM, as measured by high-performance liquid chromatography [19]. The initial homeotropic orientation of $TEM_{PAA\text{-}APBA}$ was retained at low C_g (0.1 mM; Fig. 4a(i)), but the planar orientation of 5CB was observed as C_g increased (0.3–2.5 mM; Fig. 4a(ii–vi)). This result indicates that the sensitivity of $TEM_{PAA\text{-}APBA}$ to glucose in human serum is similar to that in aqueous solution. The sensitivity of $TEM_{PAA\text{-}APBA}$ to glucose

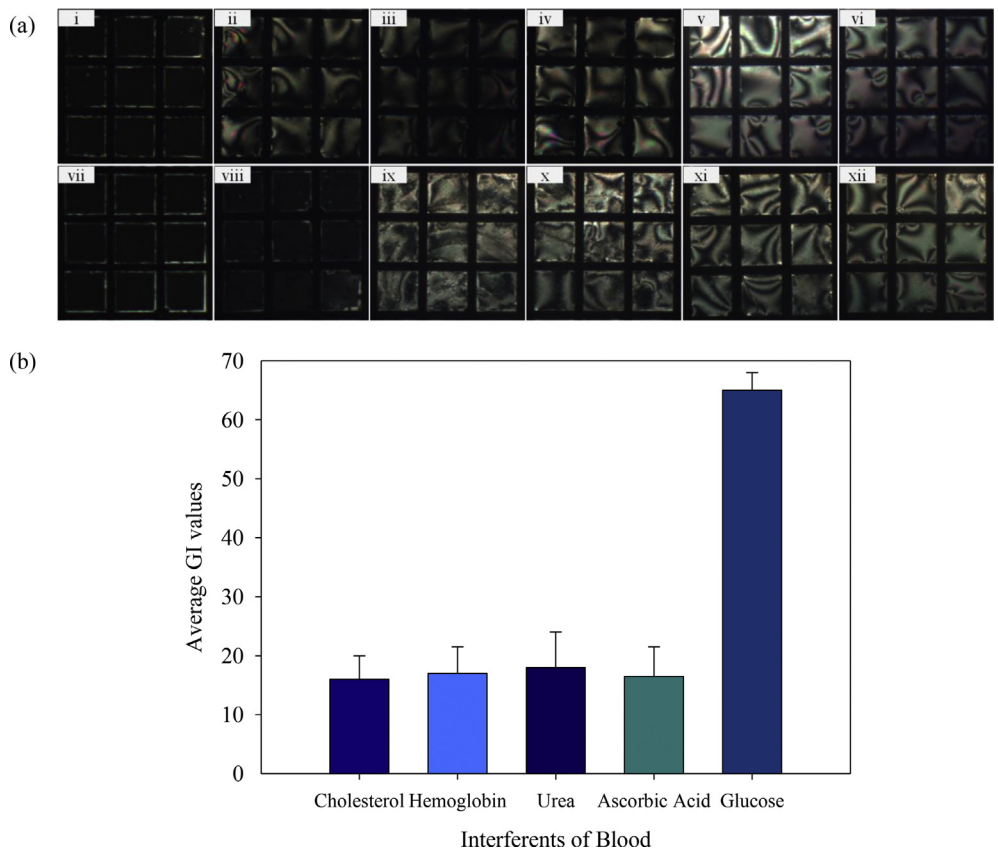

Fig. 4. (a) POM images (under crossed polarisers) of the $TEM_{PAA\text{-}APBA}$ in the diluted human serum sample at C_g = (i) 0.1, (ii) 0.3, (iii) 0.5, (iv) 0.75, (v) 1, and (vi) 2.5 mM and those in the human urine sample with the addition of glucose at C_g = (vii) 0 (pure urine sample from a non-diabetic patient), (vii) 0.05, (iiX) 0.1, (x) 0.2, (xi) 1, and (xii) 3 mM, and (b) the plot of average GI values (calculated from the raw POM images of Figure SI 2) of the $TEM_{PAA\text{-}APBA}$ after injection the major interferents of blood in the $TEM_{PAA\text{-}APBA}$ cell; the C_g was controlled by dilution with water.

Please cite this article in press as: S. Munir, S.-Y. Park, Label- and enzyme-free detection of glucose by boronic acid-coupled poly(styrene-*b*-acrylic acid) at liquid crystal/aqueous interfaces, Analytica Chimica Acta (2018), https://doi.org/10.1016/j.aca.2018.05.039

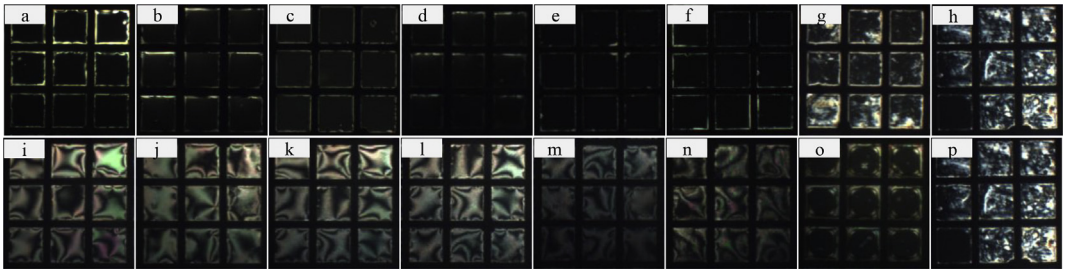

Fig. 5. POM images (under crossed polarisers) of the $TEM_{PAA-APBA}$ in the aqueous media (a–h) before and (i–p) after injection of the aqueous glucose solution (1 mM) (a, i) 5, (b, j) 10, (c, k) 15, (d, l) 20, (e, m) 25, (f, n) 30, (g, o) 35, and (h, p) 40 d after freshly prepared.

in human urine was also tested after adding glucose solution at different C_g (Fig. 4a(vii–xii)). The initial homeotropic orientation was persistent in the pure urine sample (Fig. 4a(vii)), indicating that this sample contained a small amount of glucose below the sensitivity limit (~0.1 mM). At $C_g = 0.05$ mM (Fig. 4a(vii)), the same homeotropic orientation was observed, but the orientation changed from homeotropic to planar at $C_g = 0.1–3$ mM (Fig. 4a(iix and ix)), indicating that the detection limit for glucose in human urine is similar to that in aqueous solution. Thus, $TEM_{PAA-APBA}$ can be used to sense glucose in real human blood and urine samples.

The selectivity of $TEM_{PAA-APBA}$ toward glucose was tested by examining other major analytes in blood, such as cholesterol, haemoglobin, urea, and ascorbic acid. Fig. 4b shows the GI values (calculated from the raw POM images shown in Fig. S2) of $TEM_{PAA-APBA}$ after injecting solutions of these analytes (10 μM). The initial homeotropic orientation (GI value < 20) was preserved with all the analytes except glucose (GI value > 60), indicating that $TEM_{PAA-APBA}$ exhibits high selectivity for detection of glucose in the presence of these interferents.

3.4. Stability of $TEM_{PAA-APBA}$

The stability of $TEM_{PAA-APBA}$ was studied by investigating the glucose detection performance of the sensor over time. Fig. 5 shows POM images (under crossed polarisers) of $TEM_{PAA-APBA}$ in water at various times before and after injection of an aqueous glucose solution (1 mM). The $TEM_{PAA-APBA}$ sensor maintained its initial homeotropic orientation (Fig. 5a–f) and successfully detected glucose (Fig. 5i–n) for 5 weeks (35 d). However, in the 6th week, the original homeotropic orientation was no longer maintained and small bright spots began to appear owing to desorption of PS-*b*-PAA from the 5CB/aqueous interface and/or desorption of 5CB from the TEM cell.

4. Conclusion

A TEM grid filled with 5CB on an OTS-coated glass substrate was used to construct a reliable, fast, and proton-sensitive glucose biosensor by coating commercially available PS-*b*-PAA at the LC/aqueous interface and immobilising APBA on the PAA chains through covalent bonding. This $TEM_{PAA-APBA}$ sensor could detect small amounts of glucose (up to 0.1 mM) through H-P configurational changes observed by POM under crossed polarisers. The prepared $TEM_{PAA-APBA}$ sensor showed high stability for up to 5 weeks and exhibited high selectivity toward glucose against various important interferents in human blood. The low detection limit, high stability, and highly specific glucose detection of $TEM_{PAA-APBA}$ suggest that this sensing system may be used effectively for glucose sensing without sophisticated instruments and may overcome the inherent instability drawbacks of enzymatic biosensors. Without the requirements of sophisticated instruments for glucose sensing and expensive, non-commercial LC block copolymers, this new LC-based system using commercially available PS-*b*-PAA is expected to allow the fabrication of cost-effective and highly sensitive glucose sensors for commercial applications.

Acknowledgement

This research was supported by the Kyungpook National University Bokhyeon Research Fund, 2016.

Appendix A. Supplementary data

Supplementary data related to this article can be found at https://doi.org/10.1016/j.aca.2018.05.039.

References

[1] J. Wang, Electrochemical glucose biosensors, Chem. Rev. 108 (2008) 814–825.
[2] Diabetes Blue Circle Symbol, International Diabetes Federation, 2006.
[3] Diabetes Fact Sheet, WHOI, 2013.
[4] S. Mani, V. Vediyappan, S.-M. Chen, R. Madhu, V. Pitchaimani, J.-Y. Chang, S.-B. Liu, Hydrothermal synthesis of NiWO4 crystals for high performance non-enzymatic glucose biosensors, Sci. Rep. 6 (2016) 24128.
[5] S. Park, H. Boo, T.D. Chung, Electrochemical non-enzymatic glucose sensors, Anal. Chim. Acta 556 (2006) 46–57.
[6] K.K. Naik, A. Gangan, B. Chakraborty, C.S. Rout, Superior non-enzymatic glucose sensing properties of Ag-/Au-NiCo2O4 nanosheets with insight from electronic structure simulations, Analyst 143 (2018) 571–579.
[7] M. Wang, Z. Ma, J. Li, Z. Zhang, B. Tang, X. Wang, Well-dispersed palladium nanoparticles on nickel- phosphorus nanosheets as efficient three-dimensional platform for superior catalytic glucose electro-oxidation and non-enzymatic sensing, J. Colloid Interface Sci. 511 (2018) 355–364.
[8] C.D. Ma, L. Adamiak, D.S. Miller, X. Wang, N.C. Gianneschi, N.L. Abbott, Liquid crystal interfaces programmed with enzyme-responsive polymers and surfactants, Small 11 (2015) 5747–5751.
[9] M.I. Kinsinger, B. Sun, N.L. Abbott, D.M. Lynn, Reversible control of ordering transitions at aqueous/liquid crystal interfaces using functional amphiphilic polymers, Adv. Mater. 19 (2007) 4208–4212.
[10] S. Munir, S.-Y. Park, The development of a cholesterol biosensor using a liquid crystal/aqueous interface in a SDS-included β-cyclodextrin aqueous solution, Anal. Chim. Acta 893 (2015) 101–107.
[11] X. Niu, Y. Zhong, R. Chen, F. Wang, D. Luo, Highly sensitive and selective liquid crystal optical sensor for detection of ammonia, Optic Express 25 (2017) 13549–13556.
[12] D.-Y. Lee, J.-M. Seo, W. Khan, J.A. Kornfield, Z. Kurji, S.-Y. Park, pH-responsive aqueous/LC interfaces using SGLCP-b-polyacrylic acid block copolymers, Soft Matter 6 (2010) 1964–1970.
[13] H.-G. Lee, S. Munir, S.-Y. Park, Cholesteric liquid crystal droplets for biosensors, ACS Appl. Mater. Interfaces 8 (2016) 26407–26417.
[14] M. Khan, A.R. Khan, J.-H. Shin, S.-Y. Park, A liquid-crystal-based DNA biosensor for pathogen detection, Sci. Rep. 6 (2016) 22676.
[15] M. Khan, S.-Y. Park, Liquid crystal-based proton sensitive glucose biosensor, Anal. Chem. 86 (2014) 1493–1501.
[16] M. Khan, S.-Y. Park, General Liquid-crystal droplets produced by microfluidics for urea detection, Sensor. Actuator. B: Chem. 202 (2014) 516–522.
[17] M. Khan, S.-Y. Park, Specific detection of avidin–biotin binding using liquid crystal droplets, Colloids Surf. B: Biointerfaces 127 (2015) 241–246.
[18] M. Khan, S.-Y. Park, Liquid crystal-based glucose biosensor functionalized with mixed PAA and QP4VP brushes, Biosens. Bioelectron. 68 (2015) 404–412.
[19] M. Khan, S.-Y. Park, Liquid crystal-based biosensor with backscattering

interferometry: a quantitative approach, Biosens. Bioelectron. 87 (2017) 976–983.
[20] W. Khan, J.H. Choi, G.M. Kim, S.-Y. Park, Microfluidic formation of pH responsive 5CB droplets decorated with PAA-b-LCP, Lab a Chip 11 (2011) 3493–3498.
[21] J. Kim, M. Khan, S.-Y. Park, Glucose sensor using liquid-crystal droplets made by microfluidics, ACS Appl. Mater. Interfaces 5 (2013) 13135–13139.
[22] J.-M. Seo, W. Khan, S.-Y. Park, Protein detection using aqueous/LC interfaces decorated with a novel polyacrylic acid block liquid crystalline polymer, Soft Matter 8 (2012) 198–203.
[23] S.J. Woltman, G.D. Jay, G.P. Crawford, Liquid-crystal materials find a new order in biomedical applications, Nat. Mater. 6 (2007) 929.
[24] S. Munir, I.-K. Kang, S.-Y. Park, Polyelectrolytes functionalized nematic liquid crystal-based biosensors: an overview, Trac. Trends Anal. Chem. 83 (2016) 80–94.
[25] M. Omer, M.T. Islam, M. Khan, Y.K. Kim, J.H. Lee, I.-K. Kang, S.-Y. Park, Liquid crystal-based biosensors using a strong polyelectrolyte-containing block copolymer, poly(4-cyanobiphenyl-4′-oxyundecylacrylate)-b-poly(sodium styrene sulfonate), Macromol. Res. 22 (2014) 888–894.
[26] M. Omer, M. Khan, Y.K. Kim, J.H. Lee, I.-K. Kang, S.-Y. Park, Biosensor utilizing a liquid crystal/water interface functionalized with poly(4-cyanobiphenyl-4′-oxyundecylacrylate-b-((2-dimethyl amino) ethyl methacrylate)), Colloids Surf. B: Biointerfaces 121 (2014) 400–408.
[27] M. Omer, S.-Y. Park, Preparation of QP4VP-b-LCP liquid crystal block copolymer and its application as a biosensor, Anal. Bioanal. Chem. 406 (2014) 5369–5378.
[28] W. Khan, J.H. Choi, G.M. Kimb, S.Y. Park, Microfluidic formation of pH responsive 5CB droplets decorated with PAA-b-LCP, Lab Chip 11 (2011) 3493–3498.
[29] S. Munir, S.-Y. Park, Liquid-crystal droplets functionalized with a non-enzymatic moiety for glucose sensing, Sensor. Actuator. B: Chem. 257 (2018) 579–585.
[30] B. Lego, W.G. Skene, S. Giasson, Swelling study of responsive polyelectrolyte brushes grafted from mica substrates: effect of pH, salt, and grafting density, Macromolecules 43 (2010) 4384–4393.
[31] S. Christau, T. Möller, Z. Yenice, J. Genzer, R. von Klitzing, Brush/gold nanoparticle hybrids: effect of grafting density on the particle uptake and distribution within weak polyelectrolyte brushes, Langmuir 30 (2014) 13033–13041.
[32] E.P.K. Currie, A.B. Sieval, G.J. Fleer, M.A.C. Stuart, Polyacrylic acid Brushes: surface pressure and salt-induced swelling, Langmuir 16 (2000) 8324–8333.
[33] R. Dong, M. Lindau, C.K. Ober, Dissociation behavior of weak polyelectrolyte brushes on a planar surface, Langmuir 25 (2009) 4774–4779.
[34] B. Pappin, M.J. Kiefel, T.A. Houston, Boron-carbohydrate interactions, in: C.-F. Chang (Ed.), Carbohydrates - Comprehensive Studies on Glycobiology and Glycotechnology, InTech, Rijeka, 2012, p. 03.
[35] J. Yao, P. Ji, B. Wang, H. Wang, S. Chen, Color-tunable luminescent macrofibers based on CdTe QDs-loaded bacterial cellulose nanofibers for pH and glucose sensing, Sensor. Actuator. B: Chem. 254 (2018) 110–119.
[36] K.M. Manesh, P. Santhosh, A. Gopalan, K.-P. Lee, Electrospun poly(vinylidene fluoride)/poly(aminophenylboronic acid) composite nanofibrous membrane as a novel glucose sensor, Anal. Biochem. 360 (2007) 189–195.
[37] A.I. Gopalan, N. Muthuchamy, S. Komathi, K.P. Lee, A novel multicomponent redox polymer nanobead based high performance non-enzymatic glucose sensor, Biosens. Bioelectron. 84 (2016) 53–63.

Please cite this article in press as: S. Munir, S.-Y. Park, Label- and enzyme-free detection of glucose by boronic acid-coupled poly(styrene-*b*-acrylic acid) at liquid crystal/aqueous interfaces, Analytica Chimica Acta (2018), https://doi.org/10.1016/j.aca.2018.05.039